TRIM8-driven transcriptomic profile of neural stem cells identified glioma-related nodal genes and pathways

Santina Venuto[a,b,1], Stefano Castellana[c,1], Maria Monti[d], Irene Appolloni[e], Caterina Fusilli[c], Carmela Fusco[a], Piero Pucci[d], Paolo Malatesta[e,f], Tommaso Mazza[c], Giuseppe Merla[a,*,2], Lucia Micale[a,*,2]

[a] Division of Medical Genetics, Fondazione IRCCS Casa Sollievo della Sofferenza, Viale Padre Pio, 71013, San Giovanni Rotondo, Foggia, Italy
[b] Experimental and Regenerative Medicine, University of Foggia, Via A. Gramsci, 89/91, 71122, Foggia, Italy
[c] Bioinformatics Unit, Fondazione IRCCS Casa Sollievo della Sofferenza, Viale Padre Pio, 71013, San Giovanni Rotondo, Foggia, Italy
[d] CEINGE Advanced Biotechnology, Department of Chemical Sciences, Federico II University, Via Gaetano Salvatore, 486, 80145, Napoli, Italy
[e] U.O. Medicina Rigenerativa Ospedale Policlinico San Martino, Largo R. Benzi 10, 16132 Genova, Italy
[f] Department of Experimental Medicine (DiMES), University of Genova, Via Leon Battista Alberti, 2, 16132 Genova, Italy

ARTICLE INFO

ABSTRACT

Background: We recently reported TRIM8, encoding an E3 ubiquitin ligase, as a gene aberrantly expressed in glioblastoma whose expression suppresses cell growth and induces a significant reduction of clonogenic potential in glioblastoma cell lines.

Methods: we provided novel insights on TRIM8 functions by profiling the transcriptome of TRIM8-expressing primary mouse embryonal neural stem cells by RNA-sequencing and bioinformatic analysis. Functional analysis including luciferase assay, western blot, PCR arrays, Real time quantitative PCR were performed to validate the transcriptomic data.

Results: Our study identified enriched pathways related to the neurotransmission and to the central nervous system (CNS) functions, including axonal guidance, GABA receptor, Ephrin B, synaptic long-term potentiation/depression, and glutamate receptor signalling pathways. Finally, we provided additional evidence about the existence of a functional interactive crosstalk between TRIM8 and STAT3.

Conclusions: Our results substantiate the role of TRIM8 in the brain functions through the dysregulation of genes involved in different CNS-related pathways, including JAK-STAT.

General significance: This study provides novel insights on the physiological TRIM8 function by profiling for the first time the primary Neural Stem Cell over-expressing TRIM8 by using RNA-Sequencing methodology.

1. Introduction

Despite advances in the understanding of the molecular biology of glioblastoma (GB), this cancer remains incurable. The pathogenesis of GB is complex due to its highly deregulated genome with opportunistic deletion of tumour suppressor genes, amplification, and/or mutational hyper-activation of oncogenes, which populate a network of interconnected signalling pathways [1,2].

Recently, we reported TRIM8 as a gene aberrantly expressed in glioblastoma. Ectopic TRIM8 expression suppressed cell growth and induced a significant reduction of clonogenic potential in patient's primary glioma cell lines [3]. TRIM8 encodes for an E3 ubiquitin ligase protein [4] that controls multiple physiological functions, including inflammation, cell survival, and differentiation [5–7]. TRIM8 was reported as a crucial suppressor of the cytokine signalling (SOCS)-1-interacting protein [5] and as a modulator of the molecular switch that

directs p53 toward the transcriptional activation of cell cycle arrest genes [6]. Additional studies demonstrated that TRIM8 plays a determinant role in cancer development, including primary larynx squamous cell carcinoma, renal cell carcinoma [6,8].

TRIM8 has been reported as a regulator of stemness and self-renewal capabilities of glioma stem cells through STAT3 activation [9]. STAT3 is a member of a family of seven proteins that relays signals from activated cytokine and growth factor receptors in the plasma membrane to the nucleus, where they modulate the transcription of responsive genes involved in the regulation of a variety of critical functions, including cell differentiation, proliferation, apoptosis, angiogenesis, metastasis, and immune responses [10,11]. Multiple lines of evidence place STAT3 at the centre of development, progression, and maintenance of many human tumours, including glioma [12].

Here, we provided novel insights on the physiological functions of TRIM8 by RNA-Seq profiling of primary mouse embryonal neural stem cells (eNSCs) overexpressing TRIM8. Gene expression analysis identified several enriched pathways related to neurotransmission and to the central nervous system (CNS). We reported a number of TRIM8 expression-related glioma-driving genes, which are aberrantly expressed and correlate with overall survival of glioma patients. Finally, we provided additional new data supporting the functional link between TRIM8 and STAT3 with implications in the development and progression of glioma.

2. Materials and methods

2.1. Cell lines

Murine embryonic neurospheres were established starting from E14 telencephalic progenitors obtained as described in [13]. Briefly, E14 telencephalic emispheres were dissected from the brain and dissociated in 1 ml of Trypsin/EDTA (Life Technologies) for 15 min at 37 °C. DMEM medium with 10% fetal bovine serum (Thermo Fisher Scientific) was then added and cells were mechanically dissociated with a Pasteur pipette. After centrifugation for 5 min at 500 RCF, cells were resuspended in neural stem cells medium (DMEM/F12 from Thermo Fisher Scientific, 1× B27 supplement from Thermo Fisher Scientific, 10 ng/ml EGF from Peprotech, 10 ng/ml bFGF from Peprotech) and seeded in 24 well plates (50,000–150,000 cells/well). After plating, cells were infected with replication in competent retrovirus expressing the murine FLAG-tagged Trim8 sequence and a GFP cassette or a control vector expressing only the GFP cassette. After a short period of expansion *in vitro*, infected cells were FACS-sorted to obtain a pure population of GFP-positive cells that were used for RNA-Seq analysis.

HEK293 and U87MG cell lines were maintained in DMEM with Glutamax medium supplemented with 10% fetal bovine serum and 1% antibiotics (Thermo Fisher).

2.2. Retroviral vectors

The murine FLAG-tagged Trim8 sequence was cloned in the pCAG:GFP MMLV retroviral vector (kindly provided by Dr. M. Goetz, Institute of Stem Cell Research, Germany), upstream the IRES–GFP reporter cassette. As control vector we used the same pCAG:GFP vector expressing only the IRES-GFP cassette. Replication-defective retroviral supernatants were prepared by transiently transfecting plasmids into Phoenix packaging cells and harvesting the supernatant after 2 days. The supernatants were concentrated by centrifugation and stored at −80 °C before use.

2.3. RNA-Seq library preparation and sequencing

Total RNA was extracted using mini RNase kit reagent (Qiagen) and treated with DNase-RNase free (Qiagen). RNA integrity was evaluated by using the Agilent 2100 Bioanalyzer (Agilent Technologies). Next-generation sequencing experiments were performed by Genomix4Life S.r.l. (Baronissi, Italy). Indexed libraries were prepared from purified RNA with the TruSeq Total Stranded RNA Sample Prep Kit (Illumina) according to the manufacturer's instructions. Libraries were quantified using the Agilent 2100 Bioanalyzer (Agilent Technologies). Index-tagged samples were equimolar and the overall concentration was 2 nM. The pooled samples were subject to cluster generation and sequenced using an Illumina HiSeq 2500 System (Illumina) in a 2 × 100 paired-end format at a final concentration of 8 pmol.

2.4. Pre-processing and mapping reads to the mouse reference genome

RNA-Seq yielded an average number of 68,5 million reads per sample, ranging from 60 to 86 million reads. Raw data (.fastq files) were quality-controlled using the FastQC v0.11.5 software package and exhibited an average quality score as high as 36 (phred). Reads were discarded if the average per-base phred values were < 20 or trimmed by Trimmomatic [14] if the phred values of > 5% of nucleotides at the extremities of the reads were lower than 20. Residual adapter sequences were removed by cutadapt. > 75% of the paired-end reads were mapped to the GRCm38 mouse reference genome by TopHat 2. To summarize the alignments statistics, the resulting BAM files were analysed using SAMtools.

2.5. Differential expression and survival analyses

Uniquely mapped reads were counted and RPKM-normalized. To assess the cross-sample consistency of the expression profiles, the Pearson's correlation coefficient was calculated for each pairwise combination of samples. Differential gene expression was obtained by one-way ANOVA, as implemented in Partek® Genomics Suite® version 6.6, if Benjamini-Hochberg's FDR-adjusted p-values < .05. Any random batch effect was mitigated by the Batch Effect Removal® tool of Partek.

Differentially expressed genes were subjected to Gene Set Enrichment Analysis (GSEA) by Ingenuity® Pathway Analysis (IPA®, Qiagen, Summer 2017 Release). The whole procedure of functional enrichment analysis was based on the prior calculation of the activation z-scores, by which we inferred the activation states of biological functions and pathways. An enrichment score (Fisher's exact test, p-value), instead, was calculated to measure the overlap between observed and predicted deregulated gene sets. We considered p-values < .05, with positive or negative z-scores indicating predicted activated or inhibited functions/pathways. Categories of functional annotations were ranked by a score computed with the weighted sum of the absolute z-scores of the diseases and functions belonging to the categories. Weights were calculated as the complement of the inverse of -log p-value (*pv*), as reported in [15].

Correlation of expression between functionally relevant genes and *TRIM8* was checked in The Cancer Genome Atlas (TCGA; https://cancergenome.nih.gov/) cohort of glioma tissues (530 Low Grade Gliomas and 166 Glioblastomas) through Spearman correlation test. Considering the high variability of the gene expression profiles of these tumour samples, a minimum correlation value of 0.2 was set.

The Log-Rank test was used to compare the survival distributions of two samples divided according to the mean expression values of *TRIM8* and of other relevant genes. Samples having expression levels greater than the mean value were assigned to the High group, while samples with the expression values less or equal to the mean were assigned to the Low group. All statistical computations were made through R statistical software (R version 3.3.2).

2.6. PCR arrays validation of RNA-Seq differential expressed genes

Mouse embryonic neurospheres were infected with a retrovirus expressing FLAG-Trim8 or with an empty vector. Total RNA was extracted using mini RNase kit reagent (Qiagen), treated with DNase-

RNase free (Qiagen), quantified by Nanodrop (Thermo Fisher Scientific) and reverse-transcribed using RT^2 First Strand Kit (Qiagen) according to the manufacturer's instructions. Resulting complementary DNA from each sample was aliquoted both into mouse Jak-Stat signalling RT^2 Profiler™ PCR arrays (Qiagen/SABiosciences catalog no. PAMM-039Y, gene list provided online). Real-time PCRs were performed on an ABI 7900 (Thermo Fisher Scientific-Applied Biosystems). Data were analysed by using RT^2 Profiler PCR Array data analysis software (www.SABiosciencies.com/pcrarraydataanalysis.php), provided by SABiosciences.

2.7. Quantitative real time PCR

Total RNA from mouse embryonic neurospheres infected with a retrovirus expressing FLAG-Trim8 or with an empty vector was reverse transcribed using the Quantitect Transcription kit (Qiagen), according to the manufacturer's instructions. Oligos for qPCR were designed using the Primer express program (Rozen and Skaletsky, 2000) with default parameters. *GAPDH* and *ACTIN* were used as reference genes. The reactions were run in triplicate in 10 ul of final volume with 10 ng of sample cDNA, 0.3 mM of each primer, and 1XPower SYBR Green PCR Master Mix (Termo Fisher Scientific-Applied Biosystems). Reactions were set up in a 384-well plate format with a Biomeck 2000 (Beckmann Coulter) and run in an ABI Prism7900HT (Thermo Fisher Scientific-Applied Biosystems) with default amplification conditions. Raw Ct values were obtained using SDS 2.3 (Applied Biosystems). Calculations were carried out by the comparative Ct method as reported in [16]. Significance was determined by a two-tailed unpaired *t*-test for means.

2.8. Dual-luciferase assay

HEK293 and U87MG cells were plated in 12-wells culture dishes at a density of 4×10^4 cells/ml and then co-transfected with a pNanoLuc-SIE reporter vector (Promega), pGL3-basic FireFly (Promega) and pDEST-EGFP-STAT3, p3xFLAG-TRIM8 or p3xFLAG-TRIM8 b-box deletion mutant constructs, using Lipofectamine® LTX (Thermo Fisher Scientific) according to the manufacturer's instructions. 48 h after transfection, firefly luciferase activity was monitored using the Dual-GLO® Luciferase Assay System (Promega) in a Glomax 96 microplate luminometer and was normalized to the Nano luciferase activity of the pNanoLuc-SIE vector for each transfected well.

2.9. Co-immunoprecipitation and western blot

HEK293 and U87MG cells were plated in 100 mm culture dishes at a density of 5×10^5 cells/ml, transfected with the indicated plasmids. After 48 h, cells were lysed in RIPA buffer. Total lysates cells were co-immunoprecipitated with anti-FLAG (Sigma) or anti-EGFP (Santa Cruz) using Dynabeads magnetic beads (Thermo Fisher Scientific) following manufacturer's instructions. Complexes were analysed by SDS page electrophoresis and blotted with EGFP, FLAG and STAT3 antibodies, as reported in [6]. Horseradish peroxidase conjugated anti-mouse (Santa Cruz) and anti-rabbit (Santa Cruz) antibodies and the ECL chemiluminescence system (GE Healthcare) was used for detection.

2.10. Isolation of nuclear and cytoplasmic extract

HEK293 and U87MG cells were plated in 60 mm culture dishes transfected with the indicated plasmids. After 48 h, cells were harvested and fractionated. Nuclear and cytoplasmic extraction was prepared using an NE-PER Nuclear Cytoplasmic Extraction Reagent kit (Pierce) according to the manufacturer's instruction. Protein concentrations of cytoplasmic and nuclear extracts were measured using the Pierce 660 nm protein assay (Thermo Fisher Scientific) with the GloMax Discover System (Promega). Nuclear and cytoplasmic extracts were resolved by SDS page electrophoresis and blotted with anti-STAT3

(79D7, Cell Signalling), anti-Phospho-STAT3 (Tyr705, Cell Signalling), anti-LaminB (Santa Cruz) and anti-αtubulin (Sigma).

ImageJ software was used to quantify band signal intensity. Values are expressed as fold differences relative to the endogenous STAT3 protein, set at 1.

2.11. DNA-binding assay

HEK293 cells were plated in 100 mm culture dishes at a density of 5×10^5 cells/ml, transfected with the indicated plasmids. After 48 h, cells were lysed in RIPA buffer. Protein concentrations of cell lysates were measured as described above and incubated with the immobilized STAT3 Consensus Oligonucleotide Sepharose conjugate (Stat3 Consensus oligonucleotide sequence: 5'-GATCCTTCTGGGAATTCCTAG ATC-3') (Santa Cruz, sc-2571 AC) in binding buffer, according to the manufacturer's instruction. Samples were centrifuged, washed and eluted from the beads by using Elution Buffer. SDS–PAGE was performed as reported in [17].

2.12. Cell sonication

HEK293 and U87MG cells were plated in 60 mm culture dishes and transfected with FLAG-TRIM8, EGFP-STAT3 and/or empty vectors. 48 h after transfection, cell pellets were lysed in RIPA buffer and than the suspension was sonicated with a microtip attached to UP50H sonifer, 40% amplitude, and constant power 12 times for 60 s, allowing the suspension to cool on ice for 1 min between pulses. After sonication, the spread of size fragments was checked by running 1 μl of total cell lysate on a 1% agarose gel.

3. Result and discussion

3.1. TRIM8-related transcriptomic profile

We recently described TRIM8, a nuclear E3 ubiquitin ligase, whose expression inversely correlates with glioma grade. TRIM8 restoration suppresses cell growth and induces a significant reduction of clonogenic potential in both U87MG glioblastoma and patients' primary glioma cell lines [3].

Since E3 ubiquitin ligase proteins regulate carcinogenesis through the timely control of many cellular processes such as DNA damage response, metabolism, transcription, and apoptosis [18–21] we reasoned that the TRIM8 activity might impact on cell transcriptome patterns, thereby promoting cancer development and progression. Therefore, we profiled the whole transcriptome of normal embryonic neural stem cells (eNSC) infected with a retrovirus expressing FLAG-Trim8 by using RNA-Seq. NSCs display molecular hallmarks of forebrain radial glia and can be considered as the "bona fide" healthy counterpart of glioma cells [22]. Moreover, *in vitro* culture of neural stem cells has proven to be a valuable experimental approach for exploring molecular processes in disease models of the central nervous system (CNS) [23].

RNA-Seq revealed 1365 differentially expressed transcripts of 912 genes (Fig. 1 A). 723 of them (corresponding to 648 RefSeq genes) differed significantly of at least 1.5 folds (192 upregulated transcripts of 178 genes and 531 downregulated transcripts of 470 genes) (Table S1). 80 genes, among all differentially expressed genes, resulted to significantly enrich 18 pathways by IPA analysis (Fig. 1B, Table S2). 53% of these genes (43 out of 80 genes) are related to cell-morphology, cell death and survival, with a preponderantly representation of signalling pathways related to neurotransmission and to CNS, including axonal guidance, GABA Receptor, ephrin B, synaptic long-term potentiation/depression, and glutamate receptor (Fig. 1C, Table S2). Four out of five CNS-related pathways have in common the *M-RAS* gene (NM_008624, *p*-value = .0060, FC = −1.54), which encodes for a member of the Ras family of the small GTPases expressed specifically in brain and heart (Fig. 1C, Table S2). It functions as a signal transducer in multiple
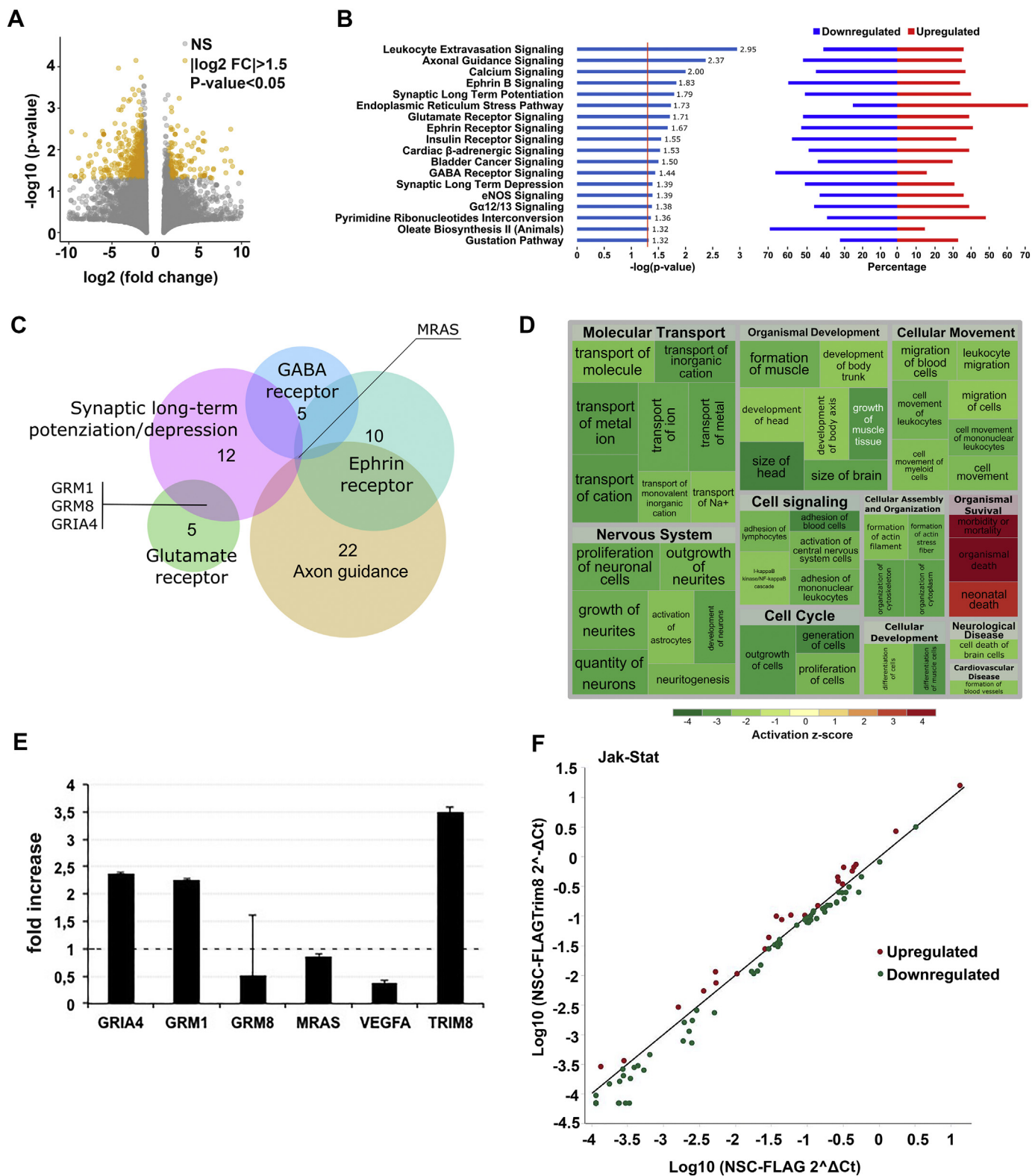
(caption on next page)

processes such as cell growth and differentiation. The dysregulation of RAS signalling plays a vital role in the oncogenesis of several cancers, including glioma [24,25]. Interestingly, *MRAS* transcriptional activation is induced by unphosphorylated STAT3 and a strong correlation between *MRAS* and *STAT3* mRNA has been reported in many cancers including colon, stomach, ovary, lung, kidney, and rectum [26].

Two out of five CNS-related pathways, the glutamate receptor and

synaptic long-term potentiation/depression signalling, share *GRM8* (NM_008174, *p*-value = .010, FC = −2.24), *GRM1* (NM_001114333, p-value = .036, FC = 8.19), and *GRIA4* (NM_0011, p-value = .044, FC = 1.68) genes. These genes encode for glutamate receptors which are highly expressed in the mammalian brain and mediate important functions in cerebellar development, synaptic plasticity, neuroprotective and neurodegenerative mechanisms (*GRM1* and *GRM8*) [27] and in

Fig. 1. TRIM8-related transcriptomic profile in neural stem cells. (A) Volcano plot of 722 differentially expressed transcripts (orange-coloured). (B) Forest plot (left) reporting 18 significantly enriched pathways, log(p-value) > 1.3; Stacked bar plot (right) accounting for proportions of upregulated and downregulated genes for each pathway. (C) EULER diagram representing the number of genes participating to five signalling pathways related to neurotransmission and to the CNS. (D) Treemap representing over-represented diseases and biological functions, grouped into processes, as calculated by IPA. Predicted activated processes are coloured in red, while inhibited processes are coloured in green, according to the inferred zs. Sizes of squares are proportional to -log(p-values). The greater a square, the more significant the enrichment of the function it corresponds to. (E) qPCR analyses were carried out on eNSC infected with a retrovirus expressing FLAG-TRIM8 or FLAG as control. Data were normalized to the expression of β-actin and L41. Bar represents the average of three replicated experiments ± standard errors. (F) The graph plots the log10 of normalized expression levels of every gene on the array in a control condition (eNSC-expressing only tag, x-axis) versus an experimental condition (eNSC-expressing FLAG-tagged Trim8, y-axis). Scatter plot: Jak-Stat PCR array, PAMM-039Y. The central line indicates unchanged gene expression. Symbols outside the delimited area indicate fold-differences larger than a threshold that we set to 1. The red symbol in the upper-left corner readily identifies up-regulated genes, and the green symbols in the lower right corner readily identify down-regulated genes. Values were derived by taking the means of fold changes of three biological replicates per time point.

fast synaptic excitatory neurotransmission (*GRIA4*) [28]. Their expression in the CNS is also regulated by the JAK-STAT signalling pathway in response to various cytokines, hormones, and growth factors [29,30].

3.2. Gene set functional enrichment analysis

Gene set enrichment analysis yielded 68 significantly represented biological functions (Fig.1D, Table S3). These line up with the classes of enriched pathways, which can be ascribed in neurological, neurotransmission, transport and cellular organization-related functions.

Among the differentially expressed genes, *VEGFA* (NM_001110268, p-value = .017, FC = −16) is the most pleiotropic gene, since it participates to 51 out of 68 biological functions (Table S3) and 4 pathways out of 18 (Table S2). VEGFA is a member of the PDGF/VEGF growth factor family that plays multiple roles in the CNS by regulating neuronal migration, angiogenesis, and axonal path finding [31–33]. VEGFA is highly expressed in glioma. Glioma cells secrete VEGFA that binds the VEGFA receptor stimulating the tumour vascular endothelial cell proliferation, migration and tube-like structure formation, and finally promotes tumour neovascularization [33,34]. This axis is mediated by a number of signalling pathways including JAK-STAT [35,36].

3.3. Validation of RNA-Seq data

RNA-Seq analysis revealed a set of genes that resulted differentially expressed. For validation we measured the expression of *GRIA4*, *GRM1*, *GRM8*, *MRAS*, and *VEGFA* genes by qPCR analysis on eNSC infected with a retrovirus expressing FLAG-Trim8, compared to that of control cells. Accordingly with the RNA-Seq data, we showed an up-regulation of *GRIA4* and *GRM1* (FC: 2.37; 2.26, respectively) and a down-regulation of *GRM8*, *MRAS*, and *VEGFA* (FC: 0.5; 0.86; 0.37, respectively) (Fig. 1E).

Our data analysis has revealed a number of pathways involving the JAK-STAT regulatory network, one of the most crucial signalling pathways implicated in the control of CNS functions by modulating the expression of genes linked to neurogenesis/gliogenesis, hormonal regulation, synaptic plasticity, and inflammation or tumorigenesis in response to hormones, growth factors or cytokines [37–39]. Consequently, dysregulation of the JAK-STAT pathway is at the heart of most brain disorders, including glioma, lesions, ischemia, neurodegenerative disorders, and epilepsies. [40].

Moreover previous reports linked TRIM8 to the JAK-STAT signalling pathway. TRIM8 plays a crucial role in controlling STAT3 activation [9,41,42] and, as many TRIM proteins, TRIM8 expression is induced by IFN that acts through JAK-STAT signalling pathway inducing the transcription of a large set of JAK-targeted genes [5].

Pathway analysis revealed perturbation of many genes related to JAK-STAT. Therefore, we verified the differential expression of a set of genes associated to JAK/STAT using a commercial PCR array. The panel of mouse genes includes nuclear co-factors, receptors and co-activators associated with the Stat proteins, Stat-inducible genes, and negative regulators of the Jak-Stat pathway.

We monitored a global dysregulation of the Jak-Stat pathway in accordance to RNA-Seq data in eNSC infected with a retrovirus expressing FLAG-Trim8, compared to control cells (Fig. 1F, S1). For instance, *Epor*, *Jak1*, and *Smad5* were found significantly down-regulated while *Stat3* up-regulated in overexpressing FLAG-Trim8 eNSC, compared to control cells, respectively. Of interest all these four genes are implicated in glioma. STAT3 is a critical mediator of tumorigenesis, tumour progression, and suppression of anti-tumour immunity in GB [43]. The pleiotropic cytokine Erythropoietin, EPO, and its receptor EPOR were aberrantly expressed in brain tumours and act as crucial factors in promoting angiogenesis in human gliomas [44]. Finally, *JAK1* and *SMAD5* were recently found up-regulated in glioma cells [45,46]. In addition, *SMAD5* was reported as a target gene of the miR-135 known to be down-regulated in GB cell lines. Forced expression of miR-135b into glioma stem cells markedly suppressed proliferation, motility and invasion of glioma cells as well as their stem cell-like phenotype through targeting *SMAD5* [47].

3.4. Correlation of CNS and glioma-related genes expression with TRIM8 in TCGA cohort

Recently, we evidenced a significant increase in the risk of death and disease progression in WHO grade III gliomas with low *TRIM8* expression levels compared to those with high mRNA levels [3].

Our expression data showed that the transcriptional levels of a number of CNS- and glioma-related genes, such as *GRIA4*, *GRM1*, *GRM8*, *EPOR*, *SMAD5*, *MRAS*, *STAT3*, and *VEGFA*, were significantly perturbed by TRIM8 expression. Therefore, we investigated whether a correlation may exist between the transcriptional level of *TRIM8* and these brain-related genes in a cohort of 530 Low Grade Glioma (LGG) and 166 Glioblastoma (GB) tissues from The Cancer Genome Atlas (TCGA) Research Network. The analysis revealed a significant positive correlation in LGG cohort between the expression of *TRIM8* and *GRIA4*, while a significant negative correlation was found between *TRIM8* and *STAT3* and *VEGFA*. With regard to the GB cohort, *TRIM8* expression positively correlates with *GRM1* and *STAT3* transcriptional levels (Fig. 2A).

In order to examine the prognostic value of combined *TRIM8* expression with the transcriptional levels of the above selected genes, we performed a survival analysis through Log-Rank test in the TCGA cohort of LGG and GB tissues.

Survival analysis estimated a significant decrease of death-risk in LGG patients with: i) high *TRIM8* expression associates to low *GRIA4* expression, compared with low *TRIM8* and low *GRIA4*; *ii*) high *TRIM8* with high *VEGFA* or *STAT3*, compared with low *TRIM8* and high *VEGFA* or *STAT3*. Analysing GB tissues, Kaplan-Meier survival curves highlighted that high *TRIM8* expression with low *STAT3*, compared with high *TRIM8* and high *STAT3*, was co-related to favorable clinical outcomes in glioma patients (Fig. 2B).

These data suggested that such expression combination might be a useful supplement to the repertoire of clinicians for predicting survival time of glioma patients and that the ability to use just one or a handful of genes to predict outcome could have an impact on therapeutic
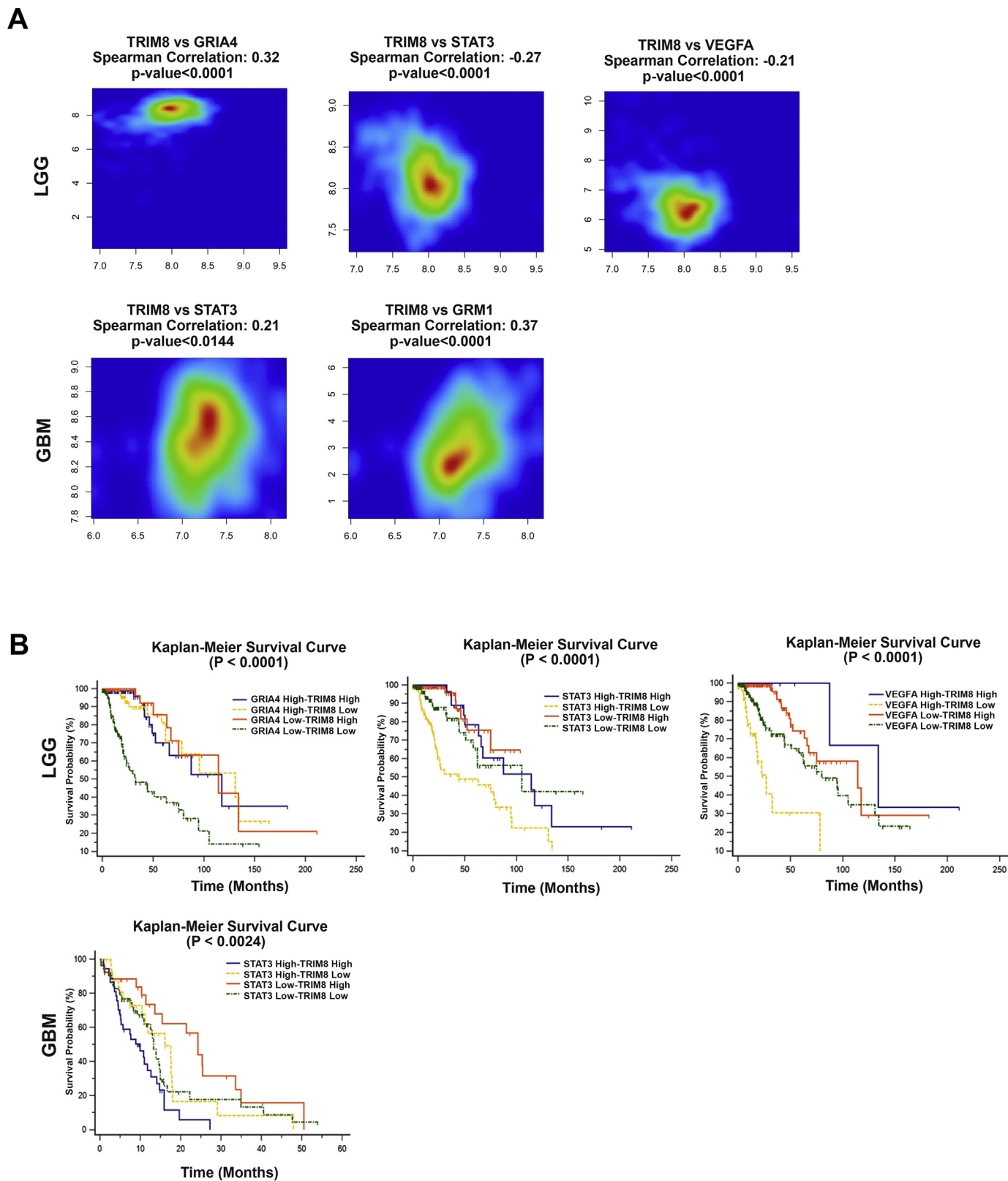
Fig. 2. Correlation of CNS and glioma-related genes expression with TRIM8 in TCGA cohort. (A) Spearman correlation between *TRIM8* and *GRIA4*, *STAT3*, *VEGFA*, and *GRM1* transcriptional levels. Graphical representation of log-transformed RPKM of 6 genes identified by RNA-Seq in a cohort of LGG and GB of The Cancer Genome Atlas Research Network (y axis) and *TRIM8* (x axis). Colours represent the density of observations at paired expression values. Higher densities are represented by red regions and lower densities are in blue, while yellow and green regions have intermediate densities that go from higher to lower, respectively. (B) Kaplan-Meier curves for Overall Survival according to RNA-Seq FPKM from LGG and GB TCGA data. We performed the Log-Rank test between the combinations of *TRIM8* expression groups and those made by other relevant genes.
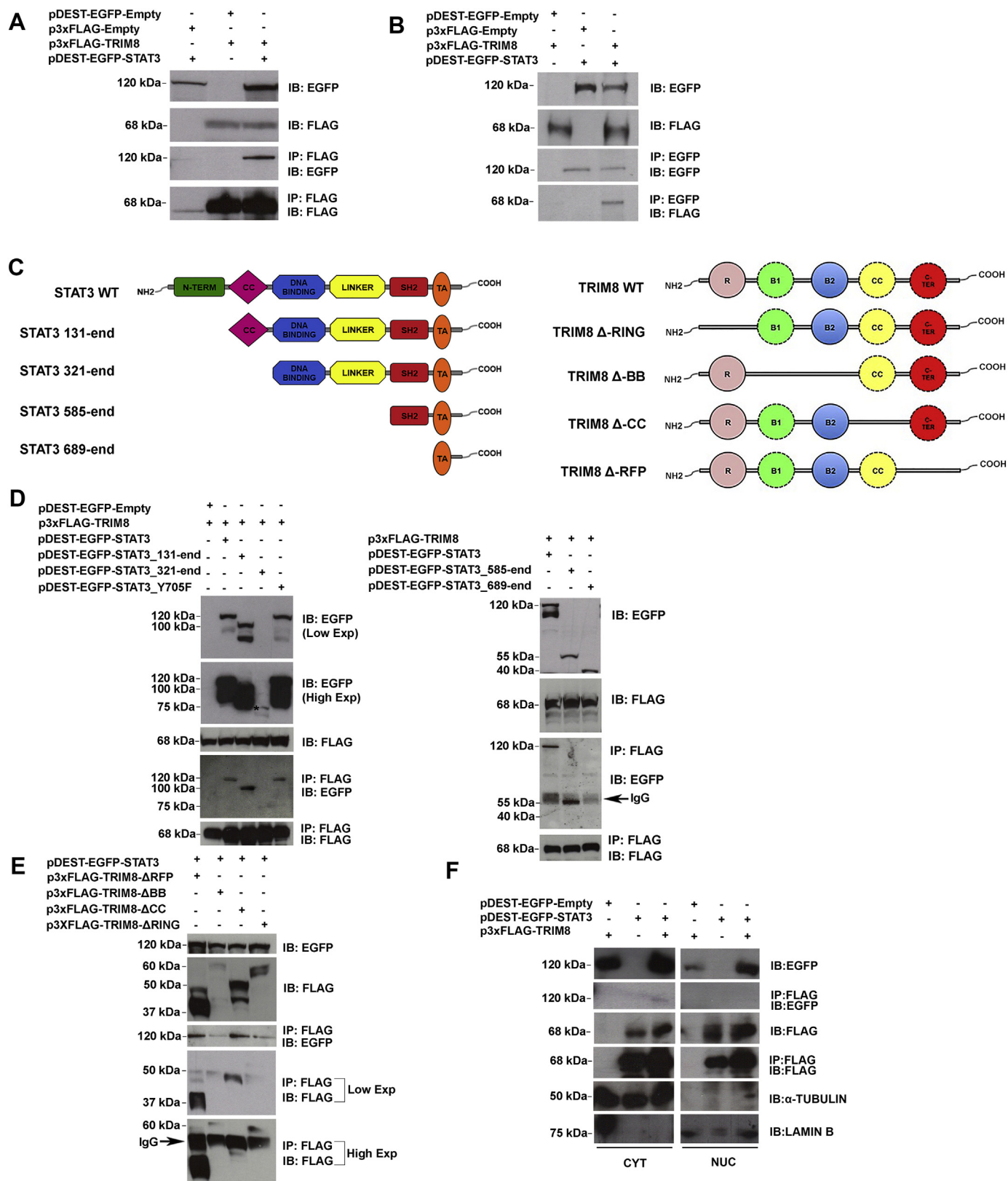
Fig. 3. TRIM8 and STAT3 self-associate (A-B) Whole protein lysates of HEK293 cells transfected with the indicated plasmids, were separated on 10% SDS-PAGE gel and subjected to immunoblotting with anti-EGFP and anti-FLAG. (C) Schematic representation of STAT3 and TRIM8 structural domains and deletion mutants (SH2: Src Homology 2; TA: transactivation; R: ring; B1-B2: BBox 1–2; CC: coiled coil; Cterm: C terminal). (D) HEK293 cells were transfected with indicated STAT3 wild type and mutants together with or without FLAG-tagged TRIM8, immunoprecipitated with anti-FLAG and followed by immunoblot as shown. (* indicates the specific band at an higher exposition time). (E) HEK293 cells were transfected with indicated plasmids encoding TRIM8 mutants together with or without EGFP-tagged STAT3. The immunoprecipitated complexes were analysed by immunoblotting with anti-EGFP and anti-FLAG (low and high exposure). (E) Whole protein lysates of HEK293 cells transfected with indicated plasmids were processed to obtain nuclear and cytoplasmic fractions, then co-immunoprecipitated with anti-FLAG; the immunocomplexes were separated on 10% SDS-PAGE gel and subjected to immunoblotting with EGFP, FLAG antibodies; Lamin B and α-tubulin antibodies were used to control nuclear and cytoplasmic fractions, respectively.
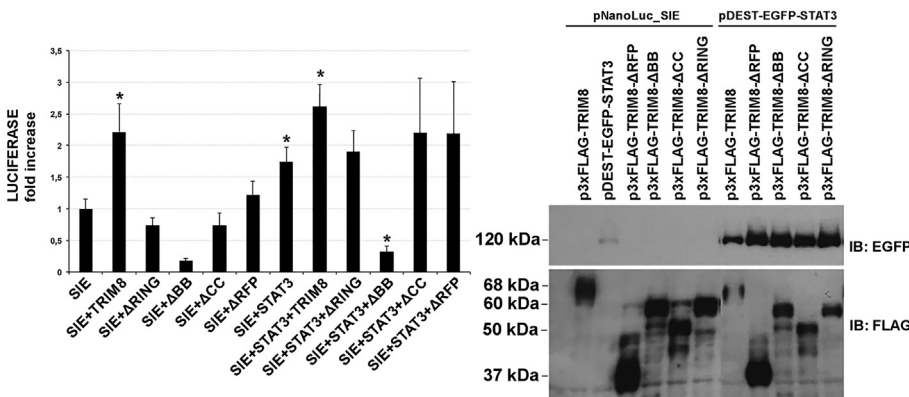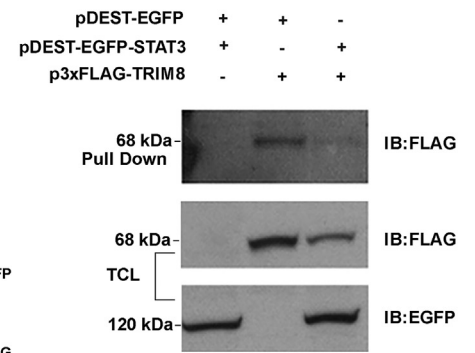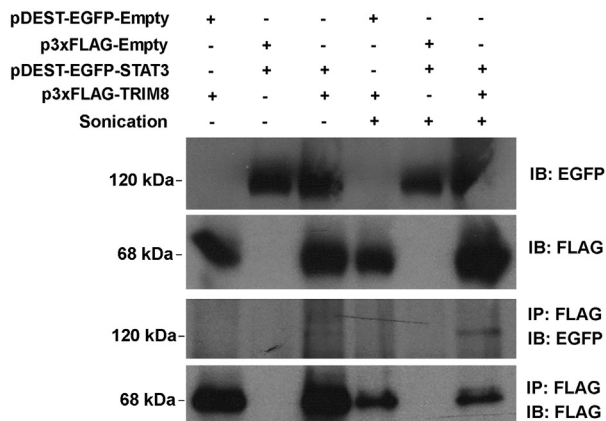
A
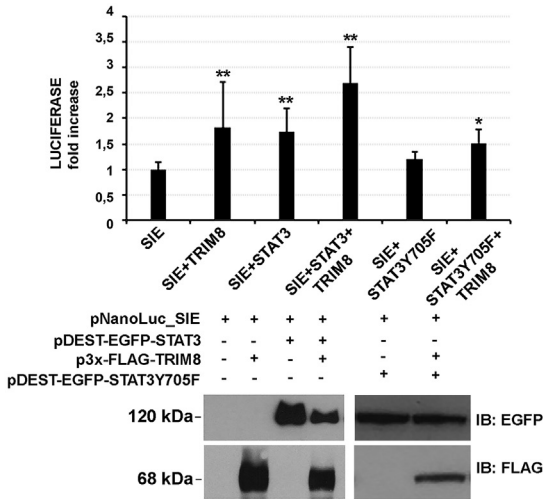
B
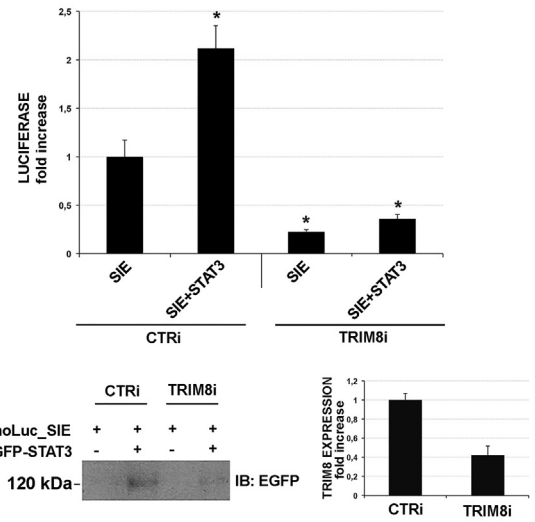
C

D

E

(caption on next page)

Fig. 4. TRIM8 interacts with STAT3 to promote STAT3 transcriptional activity directly binding SIE-sequences. (A) Luciferase assays were performed in HEK293 cells co-transfected with a pNanoLuc-SIE reporter vector, pGL3-basic FireFly and pDEST-EGFP-STAT3, p3xFLAG-TRIM8 as indicated. (B) Luciferase assays were carried out in HEK293 cells transfected with control and *TRIM8* stealths and then co-transfected with a pNanoLuc-SIE reporter vector, pGL3-basic FireFly, pDEST-EGFP-STAT3 or pDEST-EGFP-STAT3Y705F, as shown. (C) Luciferase assays were performed in HEK293 cells co-transfected with a pNanoLuc-SIE reporter vector, pGL3-basic FireFly and indicated plasmids. (A-B-C) top: luciferase activities were normalized to the level of FireFly luciferase. Each bar represents the average of three independent experiments ± standard error (**: *p* value < .01; *: p value < .05); bottom (A; B) or right (C): total lysates from HEK293 cells used for luciferase assays in C, D and E were separated on 10% SDS-PAGE gel and subjected to western blot analysis using the indicated antibodies. (D) HEK293 cells were transfected with pDEST-EGFP-STAT3, p3xFLAG-TRIM8 or empty vector and after 48 h were stimulated with IL-6 (20 ng/ml) for 30 min. To measure STAT3 and TRIM8 DNA binding, cell extracts were treated with the immobilized STAT3 Consensus Oligonucleotide (Santa Cruz)-Sepharose conjugates. The precipitates were subjected to western blot analysis with FLAG and EGFP antibodies. An aliquot of total cell lysate (TCL) was blotted with the same antibodies. (E) HEK293 cells were transfected with the indicated plasmids and harvested after 48 h. Cell lysed suspensions in lanes 4–6 were sonicated with a microtip attached to UP50H sonifier 12 times for 60 s, amplitude 40%, cycle 1. Cell lysates were then co-immunoprecipitated with anti-FLAG; the immunocomplexes were separated on 10% SDS-PAGE gel and subjected to immunoblotting with EGFP and FLAG antibodies.
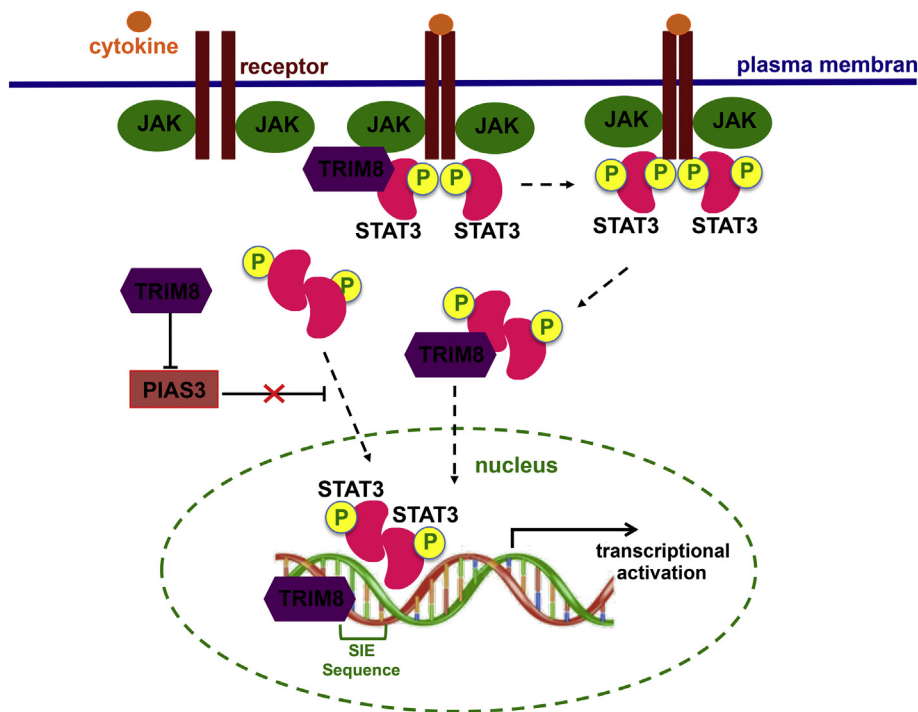

Fig. 5. Schematic model of the TRIM8 and STAT3 binding to the STAT3-responsive element in the nucleus. The model suggests that in the cytoplasmic fraction, the ectopic expression of TRIM8 may, on the one hand strengthen the ability of STAT3 to interact with JAK and on the other promote the degradation of PIAS3 through proteosomal degradation. These molecular events result in enhanced STAT3 activation and nuclear translocation. In the nucleus TRIM8 may contribute to the recruitment of STAT3 to SIE elements of a repertoire of brain disease and cancer-related genes.

treatments.

3.5. TRIM8 interacts with STAT3 to promote STAT3 transcriptional activity directly binding SIE-sequences

Experimental evidences highlighted the existence of a functional link between TRIM8 and STAT3 in several cellular contexts, including glioma stem cells [9,41,42]. Consistently we showed here that both *STAT3* and *TRIM8* expressions were significantly correlated in glioma tissues and associated to clinical outcomes in glioma patients. Therefore, based on all these evidences, we investigated the TRIM8-STAT3 loop.

Co-immunoprecipitation experiments using HEK293 and U87MG cells demonstrated that overexpressed TRIM8 and STAT3 self-associate (Fig. 3A-B; Fig. S2A, respectively). To delineate the minimal motif regions involved in TRIM8-STAT3 interaction, we used a set of STAT3 and TRIM8 deletion mutants (Fig. 3C). We found that TRIM8 interacts with all STAT3 mutants, but with the C-terminal construct expressing only the transactivation domain, from amino acid 688 to the end of the STAT3 protein, suggesting that the SH2 domain of STAT3 is required for the efficient binding of TRIM8. The physical interaction between TRIM8 and STAT3 persisted also when we used STAT3Y705F, a construct expressing a dominant-negative STAT3 mutant harbouring a substitution of tyrosine 705 to phenylalanine, which fails to be phosphorylated, suggesting that the STAT3 phosphorylation status is

dispensable for TRIM8 interaction (Fig. 3D). When we tested the TRIM8 mutants, we found that all mutants retain the ability to interact with STAT3 (Fig. 3C, E). Next, we demonstrated that TRIM8 is able to bind STAT3 in the cytoplasmic cellular compartment as revealed by co-immunoprecipitation assays performed on HEK293 and U87MG cell fractioning (Fig. 3F; Fig. S2B, respectively).

As STAT3 activity is finely regulated to ensure proper functions, TRIM8-STAT3 interaction raised the possibility that TRIM8 might modulate STAT3 transcriptional potential. To explore this, we monitored TRIM8 effect on STAT3 transcriptional activation. We performed luciferase reporter assays in HEK293 and U87MG cells using a Nano Luc vector containing the STAT3-inducible element (SIE) (NanoLuc-SIE) upstream of the luciferase reporter gene. We found a 1.7 and 1.8 significant fold increase of luciferase signal in HEK293 cells expressing exogenous STAT3 or TRIM8, respectively. Interestingly, we detected a 2.7 fold increase of reporter activation in cells co-expressing STAT3 and TRIM8 (Fig. 4A). Accordingly, we observed a 5.7 fold increase of reporter activation in U87MG cells co-expressing STAT3 and TRIM8 (Fig. S2C). Finally, the inhibition of TRIM8 expression by using specific siRNAs reduced the luciferase activity induced by STAT3 (Fig. 4B). Overall these data suggested that TRIM8 plays a role in the SIE-mediated luciferase transactivation and that its function might be mediated by endogenous STAT3. These evidences allowed us to hypothesize that TRIM8 might work together with STAT3 to potentiate the reporter activation. Next, we investigated the effects of TRIM8 domains in SIE-

binding and reporter activation by performing luciferase assays with a set of FLAG-tagged TRIM8 deletion mutants (Fig. 3C). We detected that all TRIM8 mutants partially decreased the luciferase activation both alone and when co-expressed with STAT3, suggesting the importance of TRIM8 integrity in the STAT3 activity regulation (Fig. 4C). This activity is not mediated by the nuclear STAT3Y705 phosphorylation status [48] as no changes were observed in STAT3Y705 protein level as reported on (Fig. S2D-E).

Then, we investigated whether the TRIM8 function on STAT3 transactivation is mediated by the TRIM8 binding to SIE. For this purpose, we monitored the TRIM8 presence at STAT3 consensus sequence in cellular extracts obtained from HEK293 cells containing FLAG-TRIM8 treated with and immobilized to STAT3 Consensus Oligonucleotide (Santa Cruz)-Sepharose conjugate as described previously [49]. The precipitates were subjected to western blot analysis. We detected TRIM8 bound to the STAT3 DNA-consensus in all the cellular precipitates except for that of negative control (Fig. 4D). These data supported that TRIM8 binds the STAT3 DNA-consensus.

To assess whether SIE regions participate to TRIM8-STAT3 interaction, we performed co-immunoprecipitation experiments after removing DNA from HEK293 total lysates. We found the STAT3-TRIM8 interaction still persisted, suggesting that SIE regions are not essential for the binding (Fig. 4E; Fig. S2F). All together our data demonstrated a functional link between TRIM8 and STAT3 in both HEK293 and U87MG cell lines. Although further detailed work will be required to clarify the molecular mechanisms and the physiological significance of TRIM8-STAT3 association, we may speculate that in the cytoplasmic fraction, the ectopic expression of TRIM8 may reinforce the capability of STAT3 to interact with JAK and to promote the proteosomal degradation of PIAS3 as already suggested elsewhere [41]. Consequently, these molecular events may accelerate the nuclear import of STAT3, accordingly to [42]. In the nucleus, TRIM8 may bind STAT3 inducible elements of a repertoire of brain disease and cancer-related genes probably via nuclear factors, resulting in the STAT3 activity enhancement (Fig. 5). STAT3 is a crucial convergence point of several major oncogenic signalling pathways, including those of EGFR, PDGFR, c-Met, IL-6R/gp130, cytoplasmic enzymes in the JAK family, and the Src family of kinases [50], making STAT3 an attractive molecular therapeutic target in GB. Thus, the identification of new regulators of STAT3 is crucial for novel therapeutic strategies.

4. Conclusions

The present study provides insights on the physiological functions of TRIM8 supporting some of the biological processes and the most representative molecular pathways in which *TRIM8* is involved. In particular, our results imply a role of TRIM8 in the brain functions and in gliomagenesis through the dysregulation of genes involved in pathways related to CNS, including the JAK-STAT signalling, further providing some new clues on how TRIM8 regulates STAT3 transcriptional activity.

Supplementary data to this article can be found online at https://doi.org/10.1016/j.bbagen.2018.12.001.

References

[1] E.G. Van Meir, C.G. Hadjipanayis, A.D. Norden, H.K. Shu, P.Y. Wen, J.J. Olson, Exciting new advances in neuro-oncology: the avenue to a cure for malignant glioma, CA Cancer J. Clin. 60 (3) (2010 May-Jun) 166–193.

[2] B. Vastrad, C. Vastrad, A. Godavarthi, R. Chandrashekar, Molecular mechanisms underlying gliomas and glioblastoma pathogenesis revealed by bioinformatics analysis of microarray data, Med. Oncol. 34 (11) (2017 Sep 26) 182.

[3] L. Micale, C. Fusco, A. Fontana, R. Barbano, B. Augello, P. De Nittis, et al., TRIM8 downregulation in glioma affects cell proliferation and it is associated with patients survival, BMC Cancer 15 (2015 Jun 16) 470.

[4] A. Reymond, G. Meroni, A. Fantozzi, G. Merla, S. Cairo, L. Luzi, et al., The tripartite motif family identifies cell compartments, EMBO J. 20 (9) (2001 May 1) 2140–2151.

[5] E. Toniato, X.P. Chen, J. Losman, V. Flati, L. Donahue, P. Rothman, TRIM8/GERP RING finger protein interacts with SOCS-1, J. Biol. Chem. 277 (40) (2002 Oct 4) 37315–37322.

[6] M.F. Caratozzolo, L. Micale, M.G. Turturo, S. Cornacchia, C. Fusco, F. Marzano, et al., TRIM8 modulates p53 activity to dictate cell cycle arrest, Cell Cycle 11 (3) (2012 Feb 1) 511–523.

[7] S. Hatakeyama, TRIM family proteins: roles in autophagy, immunity, and carcinogenesis, Trends Biochem. Sci. 42 (4) (2017 Apr) 297–311.

[8] M.F. Caratozzolo, A. Valletti, M. Gigante, I. Aiello, F. Mastropasqua, F. Marzano, et al., TRIM8 anti-proliferative action against chemo-resistant renal cell carcinoma, Oncotarget 5 (17) (2014 Sep 15) 7446–7457.

[9] C. Zhang, S. Mukherjee, C. Tucker-Burden, J.L. Ross, M.J. Chau, J. Kong, et al., TRIM8 regulates stemness in glioblastoma through PIAS3-STAT3, Mol. Oncol. 11 (3) (2017 Mar) 280–294.

[10] R.J. Leeman, V.W. Lui, J.R. Grandis, STAT3 as a therapeutic target in head and neck cancer, Expert. Opin. Biol. Ther. 6 (3) (2006 Mar) 231–241.

[11] D.A. Frank, STAT3 as a central mediator of neoplastic cellular transformation, Cancer Lett. 251 (2) (2007 Jun 28) 199–210.

[12] R.B. Luwor, S.S. Stylli, A.H. Kaye, The role of Stat3 in glioblastoma multiforme, J. Clin. Neurosci. 20 (7) (2013 Jul) 907–911.

[13] M. Terrile, I. Appolloni, F. Calzolari, R. Perris, E. Tutucci, P. Malatesta, PDGF-B-driven gliomagenesis can occur in the absence of the proteoglycan NG2, BMC Cancer 10 (2010 Oct 12) 550.

[14] A.M. Bolger, M. Lohse, B. Usadel, Trimmomatic: a flexible trimmer for Illumina sequence data, Bioinformatics 30 (15) (2014 Aug 1) 2114–2120.

[15] O. Palmieri, T. Mazza, A. Merla, C. Fusilli, A. Cuttitta, G. Martino, et al., Gene expression of muscular and neuronal pathways is cooperatively dysregulated in patients with idiopathic achalasia, Sci. Rep. 6 (2016 Aug 11) 31549.

[16] L. Micale, M.N. Loviglio, M. Manzoni, C. Fusco, B. Augello, E. Migliavacca, et al., A fish-specific transposable element shapes the repertoire of p53 target genes in zebrafish, PLoS One 7 (10) (2012) e46642.

[17] L. Micale, B. Augello, C. Maffeo, A. Selicorni, F. Zucchetti, C. Fusco, et al., Molecular analysis, pathogenic mechanisms, and readthrough therapy on a large cohort of Kabuki syndrome patients, Hum. Mutat. 35 (7) (2014 Jul) 841–850.

[18] R.F. Shearer, M. Iconomou, C.K. Watts, D.N. Saunders, Functional roles of the E3 ubiquitin ligase UBR5 in cancer, Mol. Cancer Res. 13 (12) (2015 Dec) 1523–1532.

[19] P. Guo, X. Ma, W. Zhao, W. Huai, T. Li, Y. Qiu, et al., TRIM31 is upregulated in hepatocellular carcinoma and promotes disease progression by inducing ubiquitination of TSC1-TSC2 complex, Oncogene 37 (4) (2018 Jan 25) 478–488.

[20] A. Mani, E.P. Gelmann, The ubiquitin-proteasome pathway and its role in cancer, J. Clin. Oncol. 23 (21) (2005 Jul 20) 4776–4789.

[21] K.I. Nakayama, K. Nakayama, Ubiquitin ligases: cell-cycle control and cancer, Nat. Rev. Cancer 6 (5) (2006 May) 369–381.

[22] H. Zong, L.F. Parada, S.J. Baker, Cell of origin for malignant gliomas and its implication in therapeutic development, Cold Spring Harb. Perspect. Biol. 29 (2015 Jan) 7(5).

[23] F.H. Gage, S. Temple, Neural stem cells: generating and regenerating the brain, Neuron 80 (3) (2013 Oct 30) 588–601.

[24] E.C. Holland, J. Celestino, C. Dai, L. Schaefer, R.E. Sawaya, G.N. Fuller, Combined activation of Ras and Akt in neural progenitors induces glioblastoma formation in mice, Nat. Genet. 25 (1) (2000 May) 55–57.

[25] L. Santarpia, S.M. Lippman, A.K. El-Naggar, Targeting the MAPK-RAS-RAF signaling pathway in cancer therapy, Expert Opin. Ther. Targets 16 (1) (2012 Jan) 103–119.

[26] J. Yang, M. Chatterjee-Kishore, S.M. Staugaitis, H. Nguyen, K. Schlessinger, D.E. Levy, et al., Novel roles of unphosphorylated STAT3 in oncogenesis and transcriptional regulation, Cancer Res. 65 (3) (2005 Feb 1) 939–947.

[27] M. Baudry, R. Greget, F. Pernot, J. Bouteiller, X. Bi, Roles of group I metabotropic glutamate receptors under physiological conditions and in neurodegeneration, WIREs Membr. Transp. Signal. 1 (2012) 523–532.

[28] M.L. MacDonald, Y. Ding, J. Newman, S. Hemby, P. Penzes, D.A. Lewis, et al., Altered glutamate protein co-expression network topology linked to spine loss in the auditory cortex of schizophrenia, Biol. Psychiatry 77 (11) (2015 Jun 1)

959–968.

[29] I.V. Lund, Y. Hu, Y.H. Raol, R.S. Benham, R. Faris, S.J. Russek, et al., BDNF selectively regulates GABAA receptor transcription by activation of the JAK/STAT pathway, Sci. Signal. 1 (41) (2008 Oct 14) ra9.

[30] D.I. Orellana, R.A. Quintanilla, C. Gonzalez-Billault, R.B. Maccioni, Role of the JAKs/STATs pathway in the intracellular calcium changes induced by interleukin-6 in hippocampal neurons, Neurotox. Res. 8 (3–4) (2005 Nov) 295–304.

[31] F. Mackenzie, C. Ruhrberg, Diverse roles for VEGF-A in the nervous system, Development 139 (8) (2012 Apr) 1371–1380.

[32] A. Quaegebeur, C. Lange, P. Carmeliet, The neurovascular link in health and disease: molecular mechanisms and therapeutic implications, Neuron 71 (3) (2011 Aug 11) 406–424.

[33] H.K. Yang, H. Chen, F. Mao, Q.G. Xiao, R.F. Xie, T. Lei, Downregulation of LRIG2 expression inhibits angiogenesis of glioma via EGFR/VEGF-A pathway, Oncol. Lett. 14 (4) (2017 Oct) 4021–4028.

[34] D.A. Reardon, S. Turner, K.B. Peters, A. Desjardins, S. Gururangan, J.H. Sampson, et al., A review of VEGF/VEGFR-targeted therapeutics for recurrent glioblastoma, J. Natl. Compr. Cancer Netw. 9 (4) (2011 Apr) 414–427.

[35] V. Cea, C. Sala, C. Verpelli, Antiangiogenic therapy for glioma, J. Signal. Transduct. 2012 (2012) 483040.

[36] J.B. Casaletto, A.I. McClatchey, Spatial regulation of receptor tyrosine kinases in development and cancer, Nat. Rev. Cancer 12 (6) (2012 May 24) 387–400.

[37] C.S. Nicolas, M. Amici, Z.A. Bortolotto, A. Doherty, Z. Csaba, A. Fafouri, et al., The role of JAK-STAT signaling within the CNS, JAKSTAT 2 (1) (2013 Jan 1) e22925.

[38] C.S. Nicolas, S. Peineau, M. Amici, Z. Csaba, A. Fafouri, C. Javalet, et al., The Jak/STAT pathway is involved in synaptic plasticity, Neuron 73 (2) (2012 Jan 26) 374–390.

[39] H. Qin, J.A. Buckley, X. Li, Y. Liu, T.H. Fox 3rd, G.P. Meares, et al., Inhibition of the JAK/STAT pathway protects against alpha-synuclein-induced neuroinflammation and dopaminergic neurodegeneration, J. Neurosci. 36 (18) (2016 May 4) 5144–5159.

[40] H.L. Grabenstatter, Y.C. Del Angel, J. Carlsen, M.F. Wempe, A.M. White, M. Cogswell, et al., The effect of STAT3 inhibition on status epilepticus and subsequent spontaneous seizures in the pilocarpine model of acquired epilepsy, Neurobiol. Dis. 62 (2014 Feb) 73–85.

[41] F. Okumura, Y. Matsunaga, Y. Katayama, K.I. Nakayama, S. Hatakeyama, TRIM8 modulates STAT3 activity through negative regulation of PIAS3, J. Cell Sci. 123 (Pt 13) (2010 Jul 1) 2238–2245.

[42] F. Okumura, A.J. Okumura, M. Matsumoto, K.I. Nakayama, S. Hatakeyama, TRIM8 regulates Nanog via Hsp90beta-mediated nuclear translocation of STAT3 in embryonic stem cells, Biochim. Biophys. Acta 1813 (10) (2011 Oct) 1784–1792.

[43] K. Swiatek-Machado, B. Kaminska, STAT signaling in glioma cells, Adv. Exp. Med. Biol. 986 (2013) 189–208.

[44] B. Nico, T. Annese, D. Guidolin, N. Finato, E. Crivellato, D. Ribatti, Epo is involved in angiogenesis in human glioma, J. Neuro-Oncol. 102 (1) (2011 Mar) 51–58.

[45] C. Du, P. Pan, Y. Jiang, Q. Zhang, J. Bao, C. Liu, Microarray data analysis to identify crucial genes regulated by CEBPB in human SNB19 glioma cells, World J. Surg. Oncol. 14 (1) (2016 Oct 6) 258.

[46] D.A. Almiron Bonnin, M.C. Havrda, M.C. Lee, H. Liu, Z. Zhang, L.N. Nguyen, et al., Secretion-mediated STAT3 activation promotes self-renewal of glioma stem-like cells during hypoxia, Oncogene 20 (2017 Nov).

[47] V. Lulli, M. Buccarelli, M. Martini, M. Signore, M. Biffoni, S. Giannetti, et al., miR-135b suppresses tumorigenesis in glioblastoma stem-like cells impairing proliferation, migration and self-renewal, Oncotarget 6 (35) (2015 Nov 10) 37241–37256.

[48] G. Huang, H. Yan, S. Ye, C. Tong, Q.L. Ying, STAT3 phosphorylation at tyrosine 705 and serine 727 differentially regulates mouse ESC fates, Stem Cells 32 (5) (2014 May) 1149–1160.

[49] Y. Sekine, S. Tsuji, O. Ikeda, M. Kakisaka, K. Sugiyama, A. Yoshimura, et al., Leukemia inhibitory factor-induced phosphorylation of STAP-2 on tyrosine-250 is involved in its STAT3-enhancing activity, Biochem. Biophys. Res. Commun. 356 (2) (2007 May 4) 517–522.

[50] T. Bowman, M.A. Broome, D. Sinibaldi, W. Wharton, W.J. Pledger, J.M. Sedivy, et al., Stat3-mediated Myc expression is required for Src transformation and PDGF-induced mitogenesis, Proc. Natl. Acad. Sci. U. S. A. 98 (13) (2001 Jun 19) 7319–7324.